Front. Chem. Sci. Eng. 2020, 14(3): 350–364
https://doi.org/10.1007/s11705-019-1894-0

REVIEW ARTICLE

A review on emulsification via microfluidic processes

Yichen Liu[1], Yongli Li (✉)[1,2], Andreas Hensel[2], Juergen J. Brandner[3], Kai Zhang[1], Xiaoze Du[1], Yongping Yang[1]

1 Key Laboratory of Condition Monitoring and Control for Power Plant Equipment (Ministry of Education), North China Electric Power University, Beijing 102206, China
2 Institute for Micro Process Engineering, Karlsruhe Institute of Technology, Eggenstein-Leopoldshafen 76344, Germany
3 Institute of Microstructure Technology, Karlsruhe Institute of Technology, Eggenstein-Leopoldshafen 76344, Germany

Abstract Emulsion is a disperse system with two immiscible liquids, which demonstrates wide applications in diverse industries. Emulsification technology has advanced well with the development of microfluidic process. Compared to conventional methods, the microfluidics-based process can produce controllable droplet size and distribution. The droplet formation or breakup is the result of combined effects resulting from interfacial tension, viscous, and inertial forces as well as the forces generated due to hydrodynamic pressure and external stimuli. In the current study, typical microfluidic systems, including microchannel array, T-shape, flow-focusing, co-flowing, and membrane systems, are reviewed and the corresponding mechanisms, flow regimes, and main parameters are compared and summarized.

Keywords microfluidics, emulsification, capillary number, droplet breakup

1 Introduction

Emulsion is defined as the dispersion of one fluid in another immiscible liquid. This process demonstrates wide applications in pharmaceutical [1–3], food [4,5], cosmetic, [6,7], petroleum [8–10], and construction industries [11]. Particularly, the monodisperse emulsion processes have gained significant attention. In the drug delivery system, a narrow distribution can provide a controlled and repeatable release process. The monodisperse emulsion process is generally used for producing microspheres, microcapsules, and microgels. When microspheres are employed as drug carriers, their small size and good monodispersity can result in less side effects, especially in case of anti-cancer agents [12]. The polymer wall of microcapsules can be sensitive to changes in environment, such as temperature or pH [13]. Microgels usually experience significant swelling or shrinking, when the external environment is changed [14], which renders the drug release controllable. In food industry, the monodisperse water-in-oil emulsion is generally adopted for encapsulating the water soluble flavors and nutrients [15]. In construction industry, stable monodisperse emulsion provides a good bond strength, when it is used as an adhesive agent for building insulation [16]. It is worth noting that monodisperse emulsion is exempt from Oswald ripening, which is highly required for maintaining long term stability [17]. In addition, the uniform physiochemical properties of individual droplets can be easily correlated to those of the dispersion system, which enables the system behavior prediction and theoretical development [18,19].

The droplet breakup techniques performed via conventional mechanical methods, such as mixing, colloid milling [20], and homogenization [21,22] are based on uneven stretching and shearing flow [23], which can easily lead to a wider distribution of droplet size and poor monodispersity. However, the microfluidics-based methods can provide better control during the preparation of monodisperse droplets. The microfluidic system limits the dimension within the range of tens to hundreds of microns. It can enhance the heat and mass transfer between the dispersed phase, continuous phase, and the inner walls of the devices [24–27]. The size, morphology, and composition of individual droplets can be more precisely controlled. The development of microfluidic emulsification technology in the past decade has remarkable. The emulsification process demonstrates a complex mechanism and is usually the result of balancing across interfacial tension forces, viscous forces, inertial forces, and forces generated due to hydrodynamic pressure and external stimuli. The droplet breakup is mainly influenced by geometric configurations and flow regimes. In this study,

Received May 4, 2019; accepted August 12, 2019

E-mail: yongli.li@ncepu.edu.cn

the emulsification process conducted via microfluidic systems is systematically studied, considering the effects of geometry, fluid properties, and operating conditions.

2 Fundamentals of droplet formation

Interfacial tension is a physical property that can significantly affect the process of droplet formation [28]. When the interface is formed, pressure difference is generated between the inside and outside of the curved interface due to the presence of interfacial tension, which is called the Laplace pressure [29] (shown in Fig. 1).

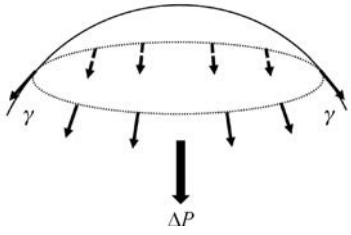

Fig. 1 Schematic of Laplace pressure.

The Laplace pressure (ΔP_{Lap}) can be calculated using the Young-Laplace equation [30]:

$$\Delta P_{\mathrm{Lap}} = \gamma\left(\frac{1}{R_1}+\frac{1}{R_2}\right), \tag{1}$$

where γ is the interfacial tension, and R_1 and R_2 are the two principal radii of the interface curvature. When the pressure generated due to all the forces other than interfacial tension force overcomes this pressure difference, the droplets would be deformed or broken. The Reynolds number (Re) describes the relative importance of inertial force to viscous force:

$$\mathrm{Re} = \frac{\rho u l}{\eta}, \tag{2}$$

where ρ is fluid density, u is the characteristic velocity, l specifies the characteristic length scale, and η is the viscosity. In most microfluidic applications, Re is relatively low [31]. The capillary number (Ca) is defined as

$$Ca = \frac{\eta U}{\gamma}, \tag{3}$$

where U is the velocity. Ca is a measure of viscous force relative to the interfacial tension force [32]. The capillary number of the continuous phase (Ca_{c}) and dispersed phase (Ca_{d}) are mainly used to characterize the flow condition in the subsequent sections.

The Rayleigh number (Ra) of the fluid is a dimensionless number associated with natural convection. It is defined as

$$Ra = \frac{\beta \Delta T l^3 g}{v\alpha}, \tag{4}$$

where β is the fluid volume expansion coefficient, ΔT is the temperature difference between the upper and lower sides of the fluid, l is the characteristic length, v is the dynamic viscosity, and α is the thermal diffusion coefficient. Ra is usually small in microsystems, because the characteristic length considered in microfluidics is in the order of 10^2 μm. For example, the Ra value of kerosene is estimated to be under 10^2, which shows that conduction dominates heat transfer, and natural convection is negligible in microsystems [33].

From the perspective of energy, droplet formation can be correlated to interface energy variation ΔG using the second law of thermodynamics as follows:

$$\Delta G = (A_2 - A_1)\gamma_{12} - T\Delta S, \tag{5}$$

where A_1 and A_2 are the surface areas before and after droplet formation, respectively. The entropy of dispersions term $T\Delta S$ is generally positive, because the droplet number increases after the breakup. In most of the cases, $(A_2–A_1)\gamma_{12} >> -T\Delta S$, and ΔG is positive, which indicates that emulsion is thermodynamically unstable [34].

3 Microfluidic emulsification systems

3.1 Microchannel array

The microchannel array emulsification has been extensively studied [35,36]. Two kinds of microchannel array systems, including the straight-through microchannel and microchannel with terrace, are reviewed in this section. The straight-through microchannel is a structure for generating emulsion using an array of uniform through-holes vertical to the plate surface [37–39], as shown in Fig. 2(a). Channel intersection was developed with two shapes that include oblong and circular [40]. The dispersed phase passed through the channel under a pressure, which was marginally higher than the breakthrough pressure. In oblong form, the interface was elongated near the tip, thereby causing instability. The continuous phase entered the space between the to-be-dispersed phase and channel wall, which was critical for spontaneous droplet formation [39]. However, in circular straight-through microchannel, the continuous phase could not enter the channel, and the droplet detachment resulted only due to the drag force from the continuous phase [41]. The droplet size varied according to the flow rate of the continuous phase, and polydisperse emulsion was formed. The aspect ratio of the slot is a crucial factor in determining whether the droplet formation is spontaneous in such designs [37].

To avoid the formation of polydisperse droplets at low flow rates, the structure microchannel with terrace (shown in Fig. 2(b)) was discovered [44]. The oil phase flows out

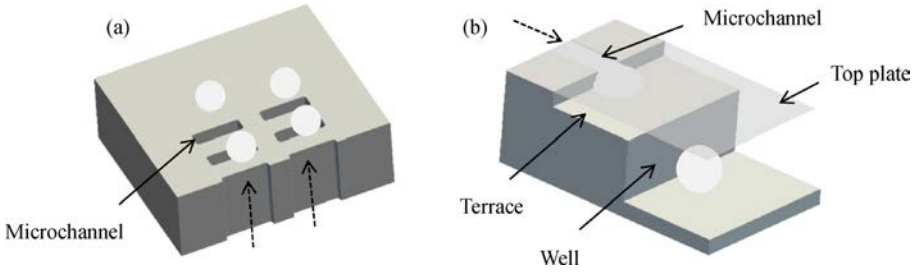

Fig. 2 Schematic of microchannel array systems (dashed lines indicate flow directions): (a) straight-through microchannel [41]; (b) microchannel with terrace [42].

of the microchannel and forms a distorted shape on the terrace. Then the dispersed phase is detached in the well, and the droplet is formed [42]. The system was delicately developed so that the interfacial area could be reduced during the droplet formation, thus rendering the interface free energy to be negative [44] and the emulsification process to be spontaneous. In the microchannel with terrace systems, when the flow rate of the dispersed phase increased to a certain extent, the droplet distribution changes from monodisperse to polydisperse, and the droplet size increased [45]. The process could be characterized by the critical *Ca* of the dispersed phase. When Ca_d was smaller than the critical value, the breakup was spontaneous and dominated by interfacial tension, the droplet size was almost constant, and the distribution was monodisperse. When Ca_d exceeded the critical value, the flow became a continuous outflow, in which the breakup was dominated by shear stress, the droplet size increased with Ca_d, and the distribution was polydisperse [46]. Therefore, maintaining the Ca_d value to be less than the critical value was important for obtaining good monodispersity.

Table 1 lists the main studies conducted in literature related to emulsification using microchannel with terrace systems. The data presented are either directly cited or calculated based on the information provided by the references [43,45,47]. The top view of the microchannel with terrace structure is presented in Fig. 3. L_{ch} and W_{ch} denote the length and the width of microchannel, respectively. L_{te} is the length of terrace, and d is the depth of microchannel and terrace. V_{cr} refers to the critical velocity of the dispersed phase, which corresponds to the aforementioned critical Ca_d value, and D is the droplet size. To facilitate the comparison, the droplet size of the emulsion produced spontaneously at low Ca_c value was considered, as it was almost constant. In group 1, both channel and terrace dimensions were changed, and the structure shape remained the same by setting $L_{te}/d \approx 7.1$, $W_{ch}/d \approx 1.2$, and $L_{ch}/d \approx 4$. It was deduced that V_{cr} was identical for all the cases, and the droplet size normalized by channel depth (D/d) remained approximately the same, which indicated that the critical velocity and normalized droplet size depended on the shape of the structures. In group 2, the dimension of the terrace was fixed, and the dimension of the microchannel was varied. It was observed during the comparison of case 2a and case 2c that when L_{ch}/d was increased from 7.6–19.4, V_{cr} increased from 1.6–2.3 mm·s^{-1}, but the produced droplet size remained constant. It was also noted during the comparison of case 2a and case 2b that when W_{ch}/d was decreased from 1.6–0.8, V_{cr} increased from 1.6–2.9 mm·s^{-1}, but the droplet size that resulted was still constant. These results established that longer and narrower microchannels increased the critical velocity and demonstrated no influence on the droplet size. In group 3, when L_{te}/d was increased from 4–10, and L_{ch}/d was increased from 15–47, V_{cr} increased from 36–158 mm·s^{-1}. Because of the lack of sufficient data, determining the correlation between L_{te}/d and V_{cr} was difficult, although the influence of L_{ch}/d on V_{cr} had been established previously. In addition, the dimension of the structure in group 3 was one order of magnitude higher than the others. However, from all the studied cases from Table 1, it is apparent that the normalized droplet size is almost the same. Therefore, it could be concluded that the droplet size depended mainly on channel depth in such structures.

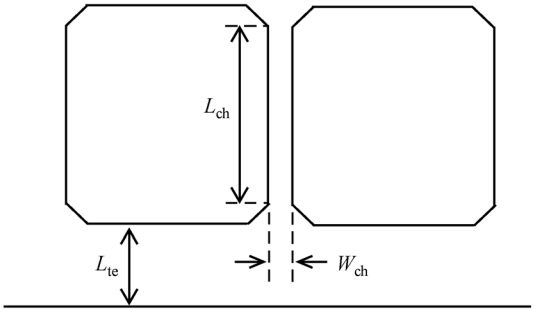

Fig. 3 Top view of the microchannel with terrace structure (L_{ch}: Length of microchannel, L_{te}: Length of terrace, W_{ch}: width of microchannel).

Figure 4 shows the correlation between D/d and Ca_d based on the experimental condition of group 1. The authors [45] varied the interfacial tension in the range of 2.9–539 mN·m^{-1}, viscosity of the dispersed phase in the

Table 1 Dimensions of the studied microchannel with terrace system, critical velocity, and droplet size of the products.

Group	Case	d /μm	L_{te} /μm	W_{ch} /μm	L_{ch} /μm	L_{te}/d	W_{ch}/d	L_{ch}/d	V_{cr} /(mm·s^{-1})	D /μm	D/d
1 [45]	1a	2	15	3.3	7.7	7.5	1.7	3.9	2.2	7	3.5
	1b	4	28	4.7	14	7.0	1.2	3.5	2.2	14	3.5
	1c	8	57	8.3	32	7.1	1.0	4	2.2	32	4
	1d	16	113	16	68	7.0	1.0	4.2	2.2	57	3.6
2 [43]	2a	7	39.3	11.6	53.1	5.6	1.6	7.6	1.6	25	3.6
	2b	7	35.6	5.9	55.6	5.1	0.8	7.9	2.9	25	3.6
	2c	7	38.4	11.3	136.1	5.5	1.6	19.4	2.3	25	3.6
3 [47]	3a	30	300	35	1400	10	1.1	47	158	100	3.3
	3b	100	400	100	1500	4	1	15	36	300	3

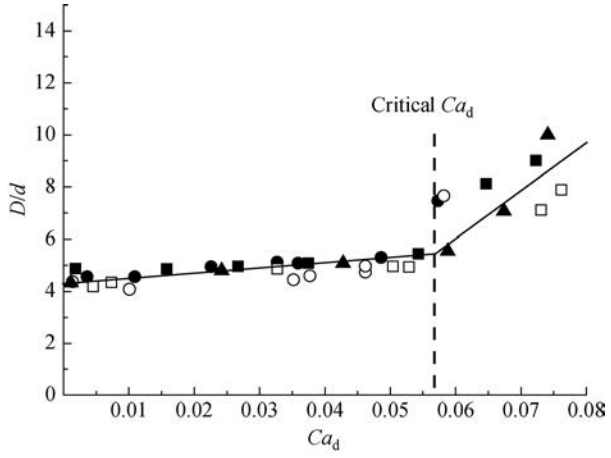

Fig. 4 Oil-in-water (O/W) emulsion through the microchannel with terrace system. Dimensionless droplet diameter (D/d) as a function of Ca_d with fixed viscosity ratio. The symbols represent droplets produced at different viscosities, channel size, and interfacial tension. Reproduced from [45] with permission, Copyright American Chemical Society, 2002.

range of 151–588 mPa·s, and the viscosity of the continuous phase in the range of 2.77–5.5 mPa·s. However, the viscosity ratio was maintained at $\eta_{d/}\eta_c \approx 56$ for all the experiments. It was established that the critical value of Ca_d was independent of interfacial tension and the viscosity of individual phase liquid. However, it was a function of viscosity ratio.

3.2 T-junction

T-junction (Fig. 5(a)) is one of the most frequently used microfluidic geometries for producing emulsions, as the droplets produced by this method can be controlled to be highly monodisperse [49–52]. The cross-flow configuration, in which the continuous phase is introduced from the horizontal channel, and dispersed phase flows through the perpendicular channel, is the most popular approach for generating droplets in T-junction [53–55]. The droplets can be formed in different locations along the main channel by varying the flow rate of the continuous phase (Q_c) or dispersed phase (Q_d). The breakup point generally corresponds to different breakup mechanisms under different flow conditions, such as squeezing, dripping, or jetting flow regimes.

In squeezing regime (shown in Fig. 5(b)), when Q_c is low, the hydrodynamic pressure, which is also called the static pressure and constitutes the hydrodynamic component in Bernoulli equation [56], increases gradually along with the inflow of the to-be-dispersed phase fluid, until the main channel is blocked [57,58]. As a result, the accumulated pressure in the continuous phase squeezes the neck of the dispersed phase, until the droplet is detached. The plug volume or normalized length (L/w) increases with an increase in the flow rate ratio of the dispersed phase to the continuous phase (Q_d/Q_c) or with a decline in the total flow rate [49,59]. The droplet deformation is not caused by shear stress, but mainly due to pressure drop, and the breakup mechanism is called "pressure-driven" [60]. The driven forces in the breakup are derived from the kinetic energy of the continuous phase fluid, wherein the normal stress is perpendicular to the interface and the shear stress is along the interface.

When Ca_c exceeds a certain value, the dripping regime (Fig. 5(c)) occurs. The critical value of Ca_c for the transition from squeezing to dripping varies due to the diversity in channel size, flow rate ratio, and viscosity ratio of both phases. For example, these values were deduced to be 0.003 [61], 0.01 [59,62], 0.1 [63], or 1 [64] in literature. In Fig. 6, when Q_d is varied from 2–8 mL·h^{-1}, the droplet size is a function of only Ca_c and independent of Q_d. In dripping regime, the necking is caused by shear stress, and the droplet breakup point is located slightly downstream from the junction. The drop volume decreases with Ca_c and shows a strong dependence on the viscosity ratio. The shear stress dominates the droplet formation process, and the correspondent breakup mechanism is called "shear-driven" [55,65]. Under this mechanism, the droplet size

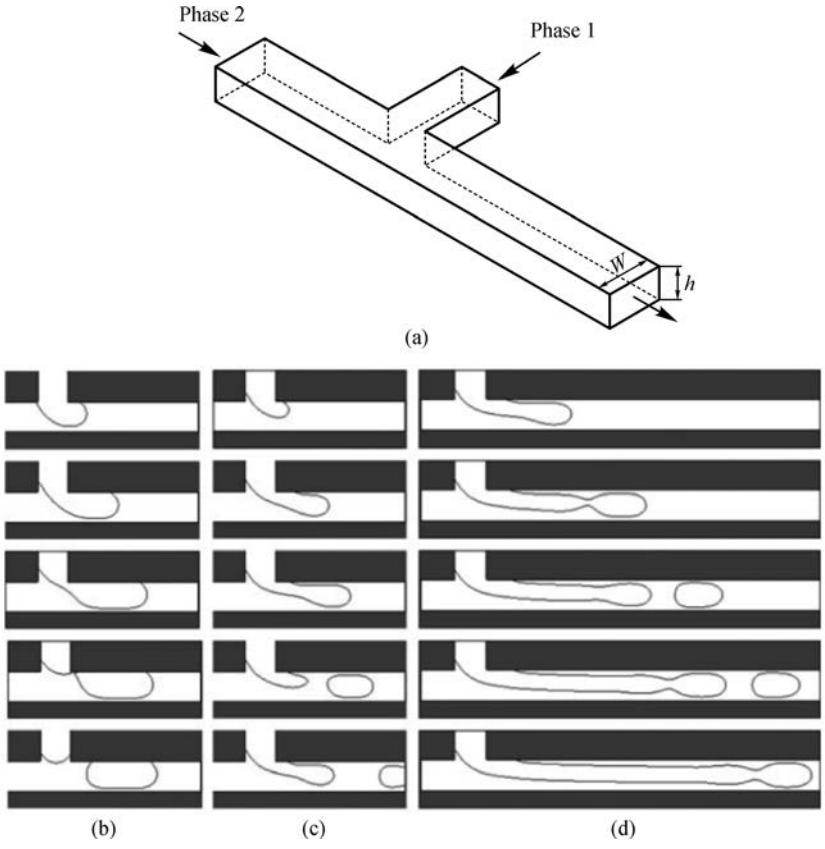

Fig. 5 T-junction with cross-flow configuration (a) structure (b) squeezing regime (c) dripping regime (d) jetting regime. Reproduced from [48] with permission, Copyright Cambridge University Press, 2008.

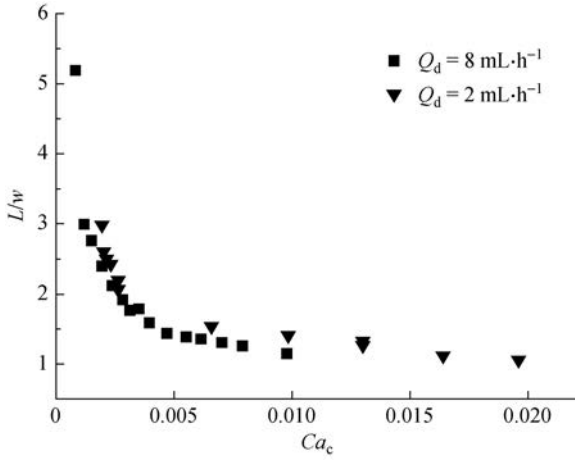

Fig. 6 Normalized plug length (L/w) as a function of Ca_c, where L is the length of the plug, and w is the width of the channel. Water-in-oil (W/O) emulsion with T-junction cross-flow (η_d = 0.58 mP·s, and η_c = 68.6 mP·s). Reproduced from [61] with permission, Copyright IOP Publishing, 2009.

can be predicted by approximately equaling the Laplace pressure with the shear stress by assuming that the droplet is a sphere [53]. However, the pressure effect cannot be completely neglected in the dripping regime [48]. Thus, it is clear that the generated droplet size resulted from the combined effects of shear stress and pressure [48], which renders the prediction of the droplet size difficult.

To realize the jetting regime (Fig. 5(d)) in T-junction, the flow rates of both phases must be sufficiently high with a well-adjusted flow ratio, until the two-phase fluids form a parallel flow. The time scales for blob formation and pinching vary with an increase in the flow rates. In jetting regime, the time scale of pinching is longer than the time scale for forming a blob, indicating that the dispersed phase flow is stretched downstream, before it is pinched off from the dispersed phase fluid [66]. In the case of jetting regime [65], the formed jet is almost stable and progressively travels downstream, which indicates the breakup resulted due to Rayleigh instability [67]. With a T-junction device, a perpendicular flow can also be configured, where the continuous phase flow is introduced from the perpendicular channel, and the dispersed flow is included from the horizontal channel. The size of the droplet obtained by perpendicular flow was not as uniform as in the one in cross-flow, and the plug length is only a function of the flow rate ratio [68].

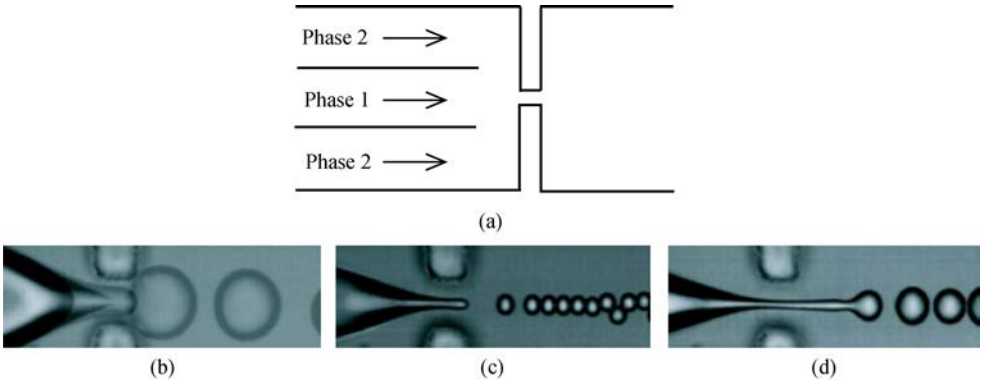

Fig. 7 Flow-focusing system (a) structure, (b) squeezing regime, (c) dripping regime and (d) jetting regime. Reproduced from [74] with permission, Copyright AIP Publishing, 2006.

3.3 Flow-focusing

The flow-focusing system is another common microfluidic device used for emulsification [69–72]. The typical flow-focusing structure is shown in Fig. 7(a). The dispersed phase flows in the intermediate channel, and the continuous phase flows in the upper and lower channels, and then both phases flow through the orifice [73]. The rupture of the dispersed phase occurs within or downstream of the orifice.

Similar to T-junction, Ca_c can be adopted in flow-focusing for characterizing the droplet breakup in different flow regimes. Ca_c is usually calculated as $Ca_c = \eta_c Ga/\gamma$. G is the effective elongation rate, and a is the radius of the parent droplet [74] or simply the half width of the dispersed phase inlet channel [75]. With an increase in Ca_c, the droplets can be formed in squeezing, dripping, or jetting regimes, as shown in Figs. 7(b–d) [76,77]. In the squeezing regime, also called the "geometry-controlled" regime [74,76], the dispersed phase from the central channel is forced into the orifice, and the flow of the continuous phase is blocked due to geometric restrictions, which is similar to the squeezing regime with T-junction. The continuous phase can only pass through the thin gap between the dispersed phase and orifice walls and generates a high pressure upstream, which drives the interface to be squeezed and deformed, until the drop is detached. Then the dispersed phase immediately fills the orifice again, and the new droplet breakup process starts [78]. The size of the produced droplet is marginally higher than the orifice diameter, and the distribution is highly monodisperse [74]. With higher Ca_c, the droplets are formed in the dripping regime. As the velocity of the continuous phase is high, the dispersed phase is concentrated in the center of the orifice and not constrained by the passage. During droplet formation, the dispersed phase remains inside or near the orifice. The droplets break up, when the dispersed phase is elongated sufficiently. It was argued that the breakup could be due to a mixed mechanism of Rayleigh instability, and shearing [79–81], because the predicted droplet size does not agree with the result estimated solely based on either of the two mechanisms. In this case, the droplets are smaller than the orifice diameter [82]. Figure 8 shows the droplet size as a function of Ca_c. It is observed from this figure that the droplet size can be reduced by increasing Ca_c or Q_c/Q_d [83]. In literature, the flow regimes have been classified differently. For example, the aforementioned squeezing regime and dripping regime can both be categorized as dripping regimes, but with different modes. The former is called the mode under rate-of-flow or pressure-driven mechanism, while the latter is called the mode under shearing or shear-driven mechanism [59]. When Ca_c increases further, the flow condition can turn into a jetting regime. The dispersed phase is extended and later broken downstream from the orifice due to Rayleigh instability, which results when the length of the jet increases to be comparable to its radius [84]. In addition, shear stress is

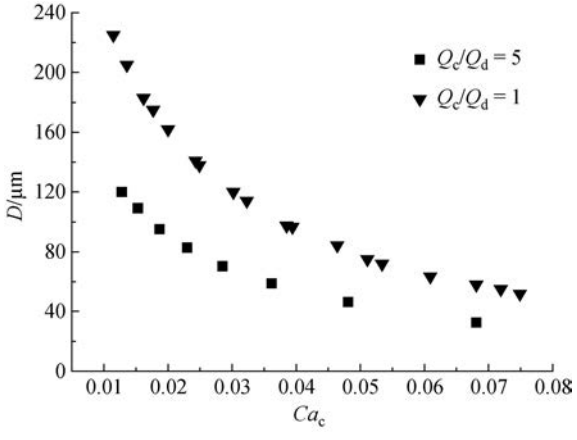

Fig. 8 Droplet size as a function of Ca_c. W/O emulsion with flow-focus. Reproduced from [83] with permission, Copyright Elsevier, 2015.

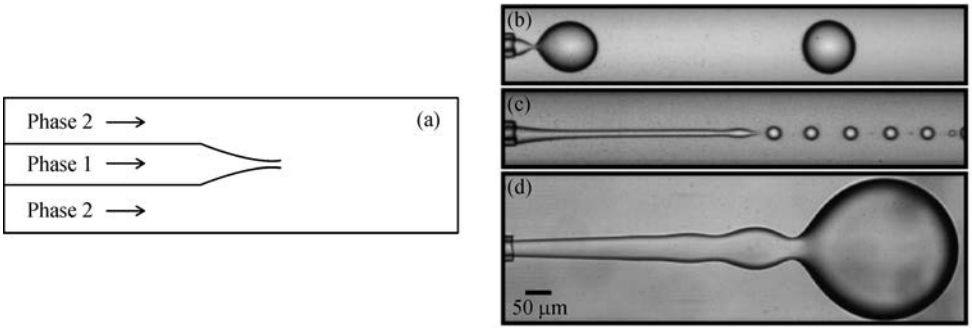

Fig. 9 Co-flowing system (a) structure, (b) dripping regime, (c) narrowing jetting, and (d) widening jetting. Reproduced from [85] with permission, Copyright American Physical Society, 2007.

exerted by the continuous phase fluid [81]. The droplet size is usually larger than the sizes of the droplets generated in the dripping mode and can be similar or even larger than the orifice dimension [74]. The distribution obtained is polydisperse.

3.4 Co-flowing

A co-flowing system is shown in Fig. 9. In a co-flowing device (shown in Fig. 9(a)), the dispersed phase is injected through a capillary or a needle in the center and flows co-currently with the continuous phase in the main channel [86,87]. The droplet can be formed either close to the tip of the capillary or detached from the jet [88–90]. Unlike the bounded flow condition, such as in the case of T-junction and flow-focusing, the effect of inertia cannot be neglected in co-flowing, as it may contribute to droplet formation. The Weber number is introduced in this section for describing the effect of the inertial force. The relationship between the inertial force and interfacial tension force can be expressed by the Weber number of the internal fluid (We_d). It is defined as follows:

$$We_d = \frac{\rho_d d U_d^{\ 2}}{\gamma}, \tag{6}$$

where ρ is the internal fluid density, U is the characteristic internal flow velocity, d is the characteristic length, and γ is the interfacial tension. The breakup in co-flowing usually occurs in dripping (Fig. 9(b)), jetting (Figs. 10(c,d)), and wavy regimes [91].

In the dripping regime, the flow rates of both continuous phase and dispersed phase are low. The droplet formation involves two steps, including the drop growth stage and separation stage [91]. In the growth stage, the viscous drag force, inertial force, and gravity force cannot overcome the interfacial tension forces. As a result, the interfacial tension dominates and holds the drop attached to the tip. The viscous drag force increases with an increase in the drop size. Then the attached drop is stretched, and a neck is formed. In the separation stage, the large local curvature

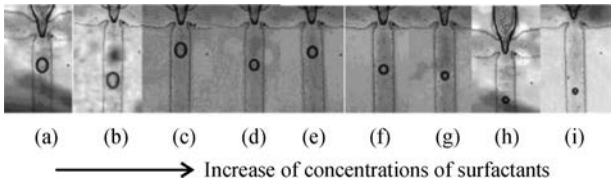

Fig. 10 Water droplet formation in flow-focusing with varied Span 80 contents: (a) 0%, (b) 0.01%, (c) 0.02%, (d) 0.05%, (e) 0.07%, (f) 0.1%, (g) 0.3%, (h) 0.5%, and (i) 6.6% (Q_c = 700 μL·h^{-1} and Q_d = 25 μL·h^{-1}). Reproduced from [105] with permission, Copyright International Society for Optics and Photonic, 2007.

leads to detachment, after which the neck shrinks rapidly [92,93].

The jetting process can be classified into narrowing jetting and widening jetting, which are characterized by different breakup mechanisms. When Q_c increases, until a critical Ca_c value is attained, the dispersed phase can be stretched as a narrowing jet form, which results in the occurrence of the narrowing jetting regime [85,91]. The velocities of the continuous phase and dispersed phase can become equal downstream along the jet [94]. The breakup of the jet is attributed to Rayleigh instability, and no clear retraction is observed after droplet detachment. Unlike narrowing jetting, widening jetting is caused, when the velocity of the dispersed phase is much higher than that of the continuous phase. The large inertial force of the dispersed phase leads to the formation of a jet. The shear force is exerted in the direction contrary to that of the dispersed phase flow at the interface, and therefore, the flow of the dispersed phase is decelerated, and the jet forms a wide head. In the widening jetting regime, discrete droplets are formed from the breakup of the jet downstream due to Rayleigh instability [85]. If the flow rate of the dispersed phase increases further, the wavy regime is formed, in which We_d of the dispersed fluid is high. For example, the wavy regime was observed, when We_d = 164 in Wu's work [91].

3.5 Membrane emulsification

Numerous studies have been conducted on Membrane emulsification (ME). Membrane emulsification can be divided into direct ME and premix ME based on whether the droplets are generated from the dispersed phase or premixed emulsion. The direct ME involves employing a low pressure difference for passing the dispersed phase through a membrane with uniform pores into the continuous phase. The premix ME can refine coarse emulsions with uneven droplet size [95]. Similar to the microchannel array emulsification, the ME process demonstrates several advantages over the traditional mechanical techniques, because it utilizes less energy, requires low shear stress, and provides products with a narrow distribution. The coefficient of variation in typical scenarios is approximately 10% [96–98]. The property of the emulsion depends strongly on the properties of the membrane [97], such as the surface wetting behavior. The hydrophilic/hydrophobic surface property of the membrane can influence the affinity between the membrane and liquid phases. The oil-in-water (O/W) or water-in-oil (W/O) emulsion can be formed, depending on whether the membrane is hydrophilic or hydrophobic [99]. The production rate can be influenced by porosity, pore size, and distance between adjacent pores. In addition to the nature of the membrane, other factors, such as flow condition, interfacial tension, and viscosity, could affect the formation of droplets during ME. When the dispersed phase attains the breakthrough pressure, the droplets are spontaneously detached due to the absence of shear flow at the membrane surface, and this type of emulsification is called the static ME. The droplets can also be formed due to shear stress, which is called the dynamic ME [95]. The dynamic ME method requires cross-flow shearing of continuous phase on the surface, where the droplets are formed. The cross-flow shearing generation can be realized either by moving the continuous phase in cross-flow, stirred, or pulsed mode, or by moving the membranes through rotation, vibration, or oscillation [96].

4 Physical properties of fluids

4.1 Interfacial tension and emulsifier

Interfacial tension represents the contracting force per unit length at the interface [100], and the interfacial tension force is one of the main forces involved in the microfluidic emulsification process. The interface consistently demonstrates the tendency to retain a small area under interfacial tension due to the effect of interfacial energy. Reducing the interfacial tension is necessary to maintain the stability of the disperse system or facilitate the emulsification. Emulsifiers or emulsifying agents are substances that are usually employed for reducing the interfacial tension [101–103]. They generally contain both hydrophilic and hydrophobic groups, which can be adsorbed at the liquid-liquid interface. Emulsifiers can be classified as ionic and nonionic surfactants, both of which demonstrate diverse emulsifying behaviors. When a new droplet is formed, the dynamic interfacial tension increases sharply. If the diffusion rate of the emulsifier molecules is adequately high to cover the newly created interface, the interfacial tension attains its equilibrium value instantaneously [104].

The emulsifier adsorbs at the interface in the form of a monolayer. When the interface adsorption attains saturation, the emulsifier molecules cannot continue to enrich on the surface and form micelles. The concentration of the emulsifier at the start of micelle formation is called the critical micelle concentration (CMC) [106,107]. The interfacial tension or interface energy can be reduced by increasing the emulsifier content, before it attains the CMC, which subsequently influences the drop size of the final product. The droplets shown in Fig. 10 were produced from a flow-focusing device. The droplet size decreases with an increase in Span 80 content in the mineral oil from 0.01%–0.3%, which corresponds to the saturated emulsifier concentration at the interface. The decrease in diameter is not significant, when the emulsifier concentration increases from 0.3%–6.6%. This is because, when the emulsifier concentration exceeds CMC, the interfacial tension of the system does not reduce further [68,108]. In the two-phase system of *n*-octane/water with sodium dodecyl sulfate as the emulsifier, the interfacial tension can be reduced to a minimum at 2.54 $mN \cdot m^{-1}$, when the concentration attains a CMC of 0.05% [68].

As the drop formation or breakup is a dynamic process, the influence of the emulsifier on the interfacial tension depends on its mass transfer behaviors, such as diffusion, sorption, and desorption [109]. The so-called “thread formation” [74] can happen in a flow-focusing system (shown in Fig. 11). In this regime, the main droplets are still produced based on the pressure-driven mechanism. However, thin threads are also formed due to the tip streaming phenomena. The elongational flow stretches the interface, resulting in the concentration gradients of emulsifiers happening along the interface with emulsifiers accumulated at the tip. This leads to a reduction in the

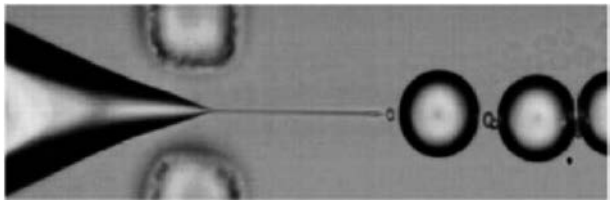

Fig. 11 Thread formation in the flow-focusing system. Reproduced from [74] with permission, Copyright AIP Publishing, 2006.

interfacial tension. Then the thread is broken into small satellite droplets. The diameter of the main drops is comparable to the size of the orifice, and the satellite drops are one order of magnitude smaller [74,76].

The emulsifying agents not only reduce the interfacial tension between water and oil, but also modify the wetting behaviors of channel walls. The adsorption of the emulsifier molecules on the interface between the fluid and channel wall can lead to a change in the contact angle [110–112]. To form an O/W or W/O emulsion, the channel walls generally need to be hydrophilic or hydrophobic. For example, when the channel wall is in contact with the water phase containing the emulsifier, the emulsifier molecules are rearranged by turning the polar heads in the water and tails onto the wall, thereby modifying the wall wetting behavior. When the emulsifier content is higher than the CMC, the wall surface is completely hydrophilic [57]. Ordered or disordered patterns are usually obtained depending on whether the wetting of the channel is complete or partial [113].

4.2 Viscosity

Viscosity is an important rheological property of the fluid. The influence of viscosity on the emulsification process is distinct for different geometries. For example, in straight-through microchannel systems producing O/W emulsion, when η_d was less than 100 mPa·s, the droplet size decreased with increasing η_d, because a high η_d value led to slow movement of the dispersed phase in the microchannel, and the resulting drop volume was low during the droplet formation time (t_f) [38], although t_f increased with an increase in η_d. In flow-focusing during O/W emulsification under the rate-of-flow mechanism, the droplet size was approximately proportional to Q_d/Q_c for low viscosity of the dispersed phase η_d (10 mPa·s). However, the correlation deviated from linear relationship for a high η_d value (500 mPa·s) [114]. This is because, in the case of low η_d, the break-up time depended on the orifice volume and Q_d, while in the case of high η_d, the neck collapse was slow, and the breakup required a longer duration, resulting in a larger droplet size than what was estimated by the linear expression. With a co-flowing system in jetting regime [85], the droplet size was affected by the drag force, when $\eta_d/\eta_c = 0.1$. However, it was independent from the velocity and determined only by the tip diameter, when $\eta_d/\eta_c >> 1$.

In general, the droplet is expected to attain a critical state of deformation, before it turns unstable and breaks up [115]. For the dispersed phase, the greater the viscosity relative to the continuous phase, the harder it is to deform [116]. It is reported that that when the viscosity ratio is greater than 4 [117], further breakup in laminar shear flow is not possible. Instead, the formation of the droplet can be still possible in laminar elongational flow. The difference between η_d and η_c contributes to the velocity profile development near the interface of the two phases [83] and is related to the flow conditions, such as shear flow or elongational flow.

The viscosity of the continuous phase can also affect the diffusion of emulsifiers. The diffusion time (τ_d) for emulsifier molecules near the droplets in laminar flow can be expressed as follows [118]:

$$\tau_d = \frac{2}{D}\left(\frac{d\Gamma}{dc}\right)^2, \tag{7}$$

where D is the diffusion coefficient of emulsifier, Γ is the adsorbed amount, and c is the concentration of the emulsifier. D can be related to viscosity using Stokes-Einstein equation as follows:

$$D = \frac{k_B T}{6\pi\eta r}, \tag{8}$$

where k_B is the Boltzmann constant, T is the absolute temperature, η is the viscosity, and r is the hydrodynamic radius. Combining Eq. (7) and Eq. (8) [104], the following relationship is obtained:

$$\tau_d \propto \eta_c. \tag{9}$$

Equation (9) indicates that the diffusion time of the emulsifier near the interface in a microfluidic system is proportional to the viscosity of the phase containing emulsifiers. The viscosity can exhibit some influence on the mass transfer behavior of the emulsifier and consequently the emulsification process. A rapid diffusion of the emulsifiers is favored for the purpose of stabilizing the emulsion, after the new interfaces are created [67].

5 Operating conditions

5.1 Flow rate

Flow rate is an important operating parameter influencing the emulsification process and can be used for adjusting the flow regimes. For example, the increase of flow rates in a confined geometry can aid in building up pressure. Similar to the viscosity difference, the flow rate difference between the dispersed and continuous phases can significantly influence the velocity profiles near the interface. The size of the produced emulsion in microfluidics can usually be correlated to flow rates or the flow rate ratio values. In the squeezing regime with T-junction cross-flow configuration, the normalized plug length (L/w) was established to be proportional to the flow rate ratio of the dispersed phase (Q_d) over continuous phase (Q_c). The relationship can be expressed as follows [58,119]:

$$L/w = \varepsilon + \delta\frac{Q_d}{Q_c}, \tag{10}$$

where L is the length of the plug, w is the width of the channel, and ε and δ are constants depending on the geometry. In Fig. 12, when Q_d/Q_c is small, the droplet size is independent of Q_d/Q_c, because the value of Q_d is very small, its marginal increase does not cause an evident change in the viscous force, and the droplet size depends only on Q_c and η_c. When Q_d/Q_c is higher, the normalized plug length fits well with Eq. (10) by substituting $\varepsilon = 1$ and $\delta = 1$ [58], which shows that L/w is a function of only Q_d/Q_c.

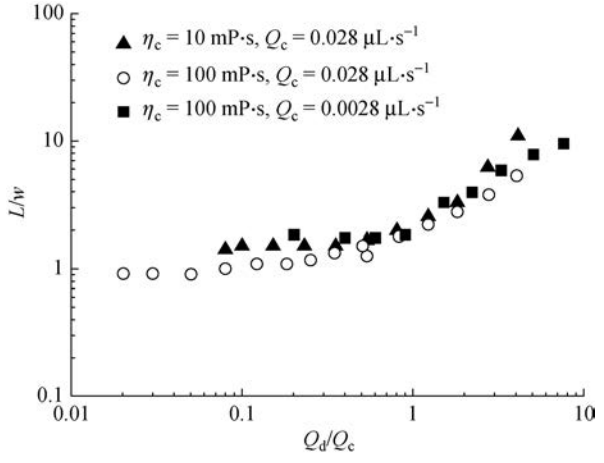

Fig. 12 Normalized length (L/w) as a function of flow rate ratio Q_d/Q_c. W/O emulsion with T-junction with cross-flow (h = 33 mm, w_c = 100 mm, and w_d = 50 mm). Reproduced from [58] with permission, Copyright Royal Society of Chemistry, 2006.

In the dripping regime with co-flowing, the droplet size increases with an increase in the velocity of the dispersed phase or decreases with an increase in the velocity of the continuous phase [88]. Thus, the dimension of the droplet can be modified by adjusting the input flow rates. In addition, the flow rate ratio can demonstrate a significant influence on droplet size distribution. For example, Hong et al. [120] studied the droplet distribution at fixed Ca_c with a co-flowing system and established that the monodisperse emulsion could only be produced, when Q_d/Q_c was over a threshold value.

5.2 Temperature

Temperature can exhibit a significant influence on the emulsification process mainly because certain physical properties of the fluids or emulsifiers are temperature-dependent. The viscosity of the liquids is caused due to continual friction between molecules located in close proximity. When the temperature is higher, the enhanced thermal motion of molecules can render the mutual friction less effective [121], which leads to a viscosity decrease and vice versa. Compared to the conventional emulsification techniques, the ability to accurately control the temperature is one of the main advantages of microsystems. By developing microstructures integrated with heat control element, the fluid viscosity can be adjusted through efficient temperature regulation during different stages of a continuous emulsification process [27]. By increasing or decreasing the temperature of the fluids before or after the breakup, the resulting viscosities can either enhance the droplet breakup or hinder the droplet coalescence, especially when the substance is highly viscous [122]. Sometimes, an unintentional temperature increase can result due to the heat converted from the mechanical energy input in the emulsification process. Therefore, controlling the temperature is beneficial for improving the quantity of the product.

When emulsifiers are involved in the disperse system, the influence of temperature on the interfacial tension is not straightforward, as the interfacial tension also depends on the physicochemical properties of the emulsifiers. For example, in soybean O/W emulsion, the interfacial tension decreases with an increase in temperature, when the nonionic emulsifier Tween 20 is used. However, it increases with an increase in the temperature, when the anionic emulsifier sodium oleate is used [123]. For the nonionic emulsifier, there exists a cloud point, over which the head groups may experience dehydration. Thus, the solubility in the aqueous phase is reduced, and CMC declines [108,124]. As a result, the ability of a nonionic emulsifier in reducing the interfacial tension is limited, which can negatively impact the emulsification process. In addition, for emulsions containing nonionic emulsifiers, there exists the phase transition temperature (PIT), above or below which the emulsifiers are dissolved in oil or aqueous phase, respectively. Thus, the O/W emulsion can be converted to W/O type with increasing temperature. PIT mainly depends on the type of oil phase [125]. The higher the solubility in the oil phase, the lower the PIT. For example, the PIT of the emulsifier polyoxyethylene nonylphenyl ether is approximately 20°C when dissolved in benzene. However, it is shifted to approximately 110°C when dissolved in hexadecane because of the low solubility [125]. It is established that when the temperature is close to PIT, the interfacial tension attains the minimum [126]. Therefore, controlling the emulsification temperature near PIT is desired for facilitating the emulsification process.

Temperature control can be implemented as a part of the emulsification system development owing to the influence of the temperature on viscosity and interfacial tension. With such a system, the droplet size can be adjusted via temperature regulation, which provides a new approach for controlling the droplet size. In the dripping regime with flow-focusing systems, if the nozzle temperature is precisely controlled, the relationship between the resultant droplet size and temperature is defined as follows:

$$D(T) \propto \frac{1}{Ca} = \frac{\gamma_c(T)}{\eta_c(T)U_c}, \quad (11)$$

where T is the temperature, D is the diameter of the droplet, and U_c is the characteristic speed of the continuous phase [127,128]. According to Eq. (11), the droplet size depends proportionally on the ratio of γ_c(T) to η_c(T). The influence of temperature on droplet size is the result of combined effects of the temperature dependences of viscosity and interfacial tension. It was reported that Nguyen et al. [129] achieved double the droplet size by increasing the temperature from 25°C–70°C, and Stan et al. [127] achieved a droplet size increase by two orders of magnitude by adjusting the temperature from 0°C–80°C.

6 Conclusions

The emulsification process achieved via microfluidic technology was briefly reviewed in this work. The droplet size and the distribution of the emulsion products were considered as the main criteria for evaluating the quality of the emulsification process. The geometric designs demonstrate a significant impact on the microfluidic emulsification process. Therefore, typical microstructured devices, including microchannel array, T-junction, flow-focusing, co-flowing, and membrane systems were systematically investigated. The droplet breakup is the result of competition between different forces, such as viscous, interfacial, and inertial forces. Generally, the droplet formation or breakup mechanisms in the aforementioned microstructures result from spontaneous transformation, pressure-driven (also called flow-of-rate), shear-driven (also called shearing), or Rayleigh capillary instability. Sometimes, the breakup process can result due to a combination of these different mechanisms. For a defined geometry, the viscosity and mass flow rates are the most important parameters that can considerably influence the force balances and velocity profiles. Emulsifiers are generally used for interfacial tension reduction, and their mass transfer kinetics can be highly affected by the viscosity of the phase, in which the emulsifier is dissolved before the droplet formation. Temperature can influence emulsification by adjusting the viscosity and interfacial tension. It can also affect the solubility of the nonionic emulsifiers. Particularly, the temperature dependence of viscosity is benefited for facilitating the breakup by stabilizing the emulsion or adjusting the droplet size. It can be expected that the innovation or optimization of microfluidic systems will be well promoted with the development of advanced manufacturing techniques [130,131] and inner surface treatment methods of microstructures. Considering the improvement achieved on microfluidic devices, process integration can also be regarded as an option.

Acknowledgements This work was supported by the National Key Research and Development Program of China (Grant Nos. 2017YFB-1103002 and 2018YFB0604304), Federal Ministry for Economic Affairs and Energy, Germany (No. 03ET1093C), Fundamental Research Funds for the Central Universities, China (No. 2017MS011), and the National Natural Science Foundation of China (Grant No. 51821004).

References

1. Zhao C X. Multiphase flow microfluidics for the production of single or multiple emulsions for drug delivery. Advanced Drug Delivery Reviews, 2013, 65(11-12): 1420–1446
2. Ran R, Sun Q, Baby T, Wibowo D, Middelberg A P, Zhao C X. Multiphase microfluidic synthesis of micro-and nanostructures for pharmaceutical applications. Chemical Engineering Science, 2017, 169: 78–96
3. Maeki M. Microfluidics for pharmaceutical applications. Microfluidics for Pharmaceutical Applications. Amsterdam: Elsevier, 2019, 101–119
4. Muijlwijk K, Berton-Carabin C, Schroën K. Cross-flow microfluidic emulsification from a food perspective. Trends in Food Science & Technology, 2016, 49: 51–63
5. Gunes D Z. Microfluidics for food science and engineering. Current Opinion in Food Science, 2018, 21: 57–65
6. Gilbert L, Picard C, Savary G, Grisel M. Rheological and textural characterization of cosmetic emulsions containing natural and synthetic polymers: Relationships between both data. Colloids and Surfaces. A, Physicochemical and Engineering Aspects, 2013, 421: 150–163
7. Ferreira A, Vecino X, Ferreira D, Cruz J, Moldes A, Rodrigues L. Novel cosmetic formulations containing a biosurfactant from *Lactobacillus paracasei.* Colloids and Surfaces. B, Biointerfaces, 2017, 155: 522–529
8. Preetika R, Mehta P S, Kaisare N S, Basavaraj M G. Kinetic stability of surfactant stabilized water-in-diesel emulsion fuels. Fuel, 2019, 236: 1415–1422
9. Sun G, Zhang J, Ma C, Wang X. Start-up flow behavior of pipelines transporting waxy crude oil emulsion. Journal of Petroleum Science Engineering, 2016, 147: 746–755
10. Zhang M, Wang W, Xie R, Ju X, Liu Z, Jiang L, Chen Q, Chu L. Controllable microfluidic strategies for fabricating microparticles using emulsions as templates. Particuology, 2016, 24: 18–31
11. Parker A P, Reynolds P A, Lewis A L, Hughes L. Semi-continuous emulsion co-polymerisation of methylmethacrylate and butylacrylate using zwitterionic surfactants as emulsifiers: Evidence of coagulative nucleation above the critical micelle concentration. Colloids and Surfaces. A, Physicochemical and Engineering Aspects, 2005, 268(1): 162–174
12. Wang L Y, Ma G H, Su Z G. Preparation of uniform sized chitosan microspheres by membrane emulsification technique and application as a carrier of protein drug. Journal of Controlled Release, 2005, 106(1-2): 62–75
13. Choi C H, Jung J H, Kim D W, Chung Y M, Lee C S. Novel one-pot route to monodisperse thermosensitive hollow microcapsules in a microfluidic system. Lab on a Chip, 2008, 8(9): 1544

14. Shah R K, Kim J W, Agresti J J, Weitz D A, Chu L Y. Fabrication of monodisperse thermosensitive microgels and gel capsules in microfluidic devices. Soft Matter, 2008, 4(12): 2303
15. Singh D, Sharma R. Post harvest wax coating of kinnow fruits to retain quality during. Storage Agricultural Engineering Today, 2007, 31(2): 232–238
16. Cameron J C, Fischer C A, Lehman N C, Lindquist J S, Olson C E, Fox S A. Hot melt adhesive pellet comprising continuous coating of pelletizing aid. US Patent, 6120899, 2000-09-19
17. Kabal'Nov A S, Pertzov A V, Shchukin E D. Ostwald ripening in two-component disperse phase systems: Application to emulsion stability. Colloids and Surfaces, 1987, 24(1): 19–32
18. Bibette J, Mason T G, Gang H, Weitz D A, Poulin P. Structure of adhesive emulsions. Langmuir, 1993, 9(12): 3352–3356
19. Mason T G. New fundamental concepts in emulsion rheology. Current Opinion in Colloid & Interface Science, 1999, 4(3): 231–238
20. Tiwary C, Kishore S, Vasireddi R, Mahapatra D, Ajayan P, Chattopadhyay K. Electronic waste recycling via cryo-milling and nanoparticle beneficiation. Materials Today, 2017, 20(2): 67–73
21. Fernández-Ávila C, Escriu R, Trujillo A. Ultra-high pressure homogenization enhances physicochemical properties of soy protein isolate-stabilized emulsions. Food Research International, 2015, 75: 357–366
22. Trujillo-Cayado L A, Alfaro M C, García M, Muñoz J. Comparison of homogenization processes for the development of green O/W emulsions formulated with *N*, *N*-dimethyldecanamide. Journal of Industrial and Engineering Chemistry, 2017, 46: 54–61
23. McClements D J. Food Emulsions: Principles, Practices, and Techniques. 3rd ed. Florida: CRC Press, 2015, 245–288
24. Squires T M, Quake S R. Microfluidics: Fluid physics at the nanoliter scale. Reviews of Modern Physics, 2005, 77(3): 977–1026
25. Geczy R, Agnoletti M, Hansen M F, Kutter J P, Saatchi K, Häfeli U O. Microfluidic approaches for the production of monodisperse, superparamagnetic microspheres in the low micrometer size range. Journal of Magnetism and Magnetic Materials, 2019, 471: 286–293
26. Li Y, Wengerter M, Gerken I, Nieder H, Scholl S, Brandner J J. Development of an efficient emulsification process using miniaturized process engineering equipment. Chemical Engineering Research & Design, 2016, 108: 23–29
27. Li Y, Gerken I, Hensel A, Kraut M, Brandner J J. Development of a continuous emulsification process for a highly viscous dispersed phase using microstructured devices. Green Processing and Synthesis, 2013, 2(5): 499–507
28. Wennerstrom H, Balogh J, Olsson U. Interfacial tensions in microemulsions. Colloids and Surfaces A—Physicochemical and Engineering Aspects, 2006, 291(1-3): 69–77
29. Diez J, Gratton R, Thomas L, Marino B. Laplace pressure-driven drop spreading: Quasi-self-similar solution. Journal of Colloid and Interface Science, 1994, 168(1): 15–20
30. Lyklema J. Fundamentals of Interface and Colloid Science. 1st ed. Amsterdam: Elsevier, 2005, 1.1–1.1.6
31. Kenis P J A, Ismagilov R F, Whitesides G M. Microfabrication inside capillaries using multiphase laminar flow patterning. Science, 1999, 285(5424): 83–85
32. Stone H A. Dynamics of drop deformation and breakup in viscous fluids. Annual Review of Fluid Mechanics, 1994, 26(1): 65–102
33. Stewart W E Jr, Dona C L G. Low Rayleigh number flow in a heat generating porous media. International Communications in Heat and Mass Transfer, 1986, 13(3): 281–294
34. Tadros T, Izquierdo P, Esquena J, Solans C. Formation and stability of nano-emulsions. Advances in Colloid and Interface Science, 2004, 108-109: 303–318
35. Kawakatsu T, Kikuchi Y, Nakajima M. Regular-sized cell creation in microchannel emulsification by visual microprocessing method. Journal of the American Oil Chemists' Society, 1997, 74(3): 317–321
36. Kawakatsu T, Komori H, Nakajima M, Kikuchi Y, Yonemoto T. Production of monodispersed oil-in-water emulsion using cross-flow-type silicon microchannel plate. Journal of Chemical Engineering of Japan, 1999, 32(2): 241–244
37. Kobayashi I, Takano T, Maeda R, Wada Y, Uemura K, Nakajima M. Straight-through microchannel devices for generating monodisperse emulsion droplets several microns in size. Microfluidics and Nanofluidics, 2008, 4(3): 167–177
38. Kobayashi I, Uemura K, Nakajima M. CFD analysis of generation of soybean oil-in-water emulsion droplets using rectangular straight-through microchannels. Food Science and Technology Research, 2007, 13(3): 187–192
39. Kobayashi I, Mukataka S, Nakajima M. Effect of slot aspect ratio on droplet formation from silicon straight-through microchannels. Journal of Colloid and Interface Science, 2004, 279(1): 277–280
40. Kobayashi I, Nakajima M, Nabetani H, Kikuchi Y, Shohno A, Satoh K. Preparation of micron-scale monodisperse oil-in-water microspheres by microchannel emulsification. Journal of the American Oil Chemists' Society, 2001, 78(8): 797–802
41. Kobayashi I, Nakajima M, Chun K, Kikuchi Y, Fukita H. Silicon array of elongated through-holes for monodisperse emulsion droplets. AIChE Journal. American Institute of Chemical Engineers, 2002, 48(8): 1639–1644
42. Sugiura S, Nakajima M, Tong J H, Nabetani H, Seki M. Preparation of monodispersed solid lipid microspheres using a microchannel emulsification technique. Journal of Colloid and Interface Science, 2000, 227(1): 95–103
43. Sugiura S, Nakajima M, Seki M. Effect of channel structure on microchannel emulsification. Langmuir, 2002, 18(15): 5708–5712
44. Sugiura S, Nakajima M, Iwamoto S, Seki M. Interfacial tension driven monodispersed droplet formation from microfabricated channel array. Langmuir, 2001, 17(18): 5562–5566
45. Sugiura S, Nakajima M, Kumazawa N, Iwamoto S, Seki M. Characterization of spontaneous transformation-based droplet formation during microchannel emulsification. Journal of Physical Chemistry B, 2002, 106(36): 9405–9409
46. Sugiura S, Nakajima M, Seki M. Preparation of monodispersed emulsion with large droplets using microchannel emulsification. Journal of the American Oil Chemists' Society, 2002, 79(5): 515–519
47. Treesuwan W, Neves M A, Uemura K, Nakajima M, Kobayashi I. Preparation characteristics of monodisperse oil-in-water emulsions by microchannel emulsification using different essential oils. LWT,

2017, 84: 617–625
48. De Menech M, Garstecki P, Jousse F, Stone H A. Transition from squeezing to dripping in a microfluidic T-shaped junction. Journal of Fluid Mechanics, 2008, 595: 141–161
49. Okushima S, Nisisako T, Torii T, Higuchi T. Controlled production of monodisperse double emulsions by two-step droplet breakup in microfluidic devices. Langmuir, 2004, 20(23): 9905–9908
50. Xu Q Y, Nakajima M. The generation of highly monodisperse droplets through the breakup of hydrodynamically focused microthread in a microfluidic device. Applied Physics Letters, 2004, 85(17): 3726–3728
51. Xu J H, Li S W, Tan J, Wang Y J, Luo G S. Controllable preparation of monodisperse O/W and W/O emulsions in the same microfluidic device. Langmuir, 2006, 22(19): 7943–7946
52. Mora A E M, de Lima e Silva A L F, de Lima e Silva S M M. Numerical study of the dynamics of a droplet in a T-junction microchannel using OpenFOAM. Chemical Engineering Science, 2019, 196: 514–526
53. Thorsen T, Roberts R W, Arnold F H, Quake S R. Dynamic pattern formation in a vesicle-generating microfluidic device. Physical Review Letters, 2001, 86(18): 4163–4166
54. Zheng B, Ismagilov R F. A microfluidic approach for screening submicroliter volumes against multiple reagents by using preformed arrays of nanoliter plugs in a three-phase liquid/liquid/gas flow. Angewandte Chemie International Edition, 2005, 44(17): 2520–2523
55. Günther A, Khan S A, Thalmann M, Trachsel F, Jensen K F. Transport and reaction in microscale segmented gas-liquid flow. Lab on a Chip, 2004, 4(4): 278–286
56. Sabri F, Lakis A A. Hydroelastic vibration of partially liquid-filled circular cylindrical shells under combined internal pressure and axial compression. Aerospace Science and Technology, 2011, 15 (4): 237–248
57. Xu J H, Li S W, Tan J, Wang Y J, Luo G S. Preparation of highly monodisperse droplet in a T-junction microfluidic device. AIChE Journal. American Institute of Chemical Engineers, 2006, 52(9): 3005–3010
58. Garstecki P, Fuerstman M J, Stone H A, Whitesides G M. Formation of droplets and bubbles in a microfluidic T-junction—scaling and mechanism of break-up. Lab on a Chip, 2006, 6(3): 437–446
59. Zhao C X, Middelberg A P J. Two-phase microfluidic flows. Chemical Engineering Science, 2011, 66(7): 1394–1411
60. Stone H A, Stroock A D, Ajdari A. Engineering flows in small devices: Microfluidics toward a lab-on-a-chip. Annual Review of Fluid Mechanics, 2004, 36(1): 381–411
61. Oishi M, Kinoshita H, Fujii T, Oshima M. Confocal micro-PIV measurement of droplet formation in a T-shaped micro-junction. Journal of Physics: Conference Series, 2009, 147: 012061
62. De Menech M, Garstecki P, Jousse F, Stone H. Transition from squeezing to dripping in a microfluidic T-shaped junction. Journal of Fluid Mechanics, 2008, 595: 141–161
63. Van der Graaf S, Steegmans M, Van Der Sman R, Schroën C, Boom R. Droplet formation in a T-shaped microchannel junction: A model system for membrane emulsification. Colloids and Surfaces. A, Physicochemical and Engineering Aspects, 2005, 266(1-3): 106–116
64. Oishi M, Kinoshita H, Oshima M, Fujii T. Investigation of micro droplet formation in a T-shaped junction using multicolor confocal micro PIV. In: Proceedings of MNHT2008. ASME, 2008, 297–301
65. Li X B, Li F C, Yang J C, Kinoshita H, Oishi M, Oshima M. Study on the mechanism of droplet formation in T-junction microchannel. Chemical Engineering Science, 2012, 69(1): 340–351
66. Seemann R, Brinkmann M, Pfohl T, Herminghaus S. Droplet based microfluidics. Reports on Progress in Physics, 2012, 75(1): 016601
67. Rayleigh L. On the capillary phenomena of jets. Proceedings of the Royal Society of London, 1879, 29(196-199): 71–97
68. Xu J H, Luo G S, Li S W, Chen G G. Shear force induced monodisperse droplet formation in a microfluidic device by controlling wetting properties. Lab on a Chip, 2006, 6(1): 131–136
69. Lignel S, Salsac A V, Drelich A, Leclerc E, Pezron I. Water-in-oil droplet formation in a flow-focusing microsystem using pressure- and flow rate-driven pumps. Colloids and Surfaces. A, Physicochemical and Engineering Aspects, 2017, 531: 164–172
70. Hamlington B D, Steinhaus B, Feng J J, Link D, Shelley M J, Shen A Q. Liquid crystal droplet production in a microfluidic device. Liquid Crystals, 2007, 34(7): 861–870
71. Yobas L, Martens S, Ong W L, Ranganathan N. High-performance flow-focusing geometry for spontaneous generation of monodispersed droplets. Lab on a Chip, 2006, 6(8): 1073–1079
72. Moon B U, Abbasi N, Jones S G, Hwang D K, Tsai S S. Water-in-water droplets by passive microfluidic flow focusing. Analytical Chemistry, 2016, 88(7): 3982–3989
73. Anna S L, Bontoux N, Stone H A. Formation of dispersions using "flow focusing" in microchannels. Applied Physics Letters, 2003, 82(3): 364–366
74. Anna S L, Mayer H C. Microscale tipstreaming in a microfluidic flow focusing device. Physics of Fluids, 2006, 18(12): 121512
75. Lee W, Walker L M, Anna S L. Impact of viscosity ratio on the dynamics of droplet breakup in a microfluidic flow focusing device. In: Co A, Leal L G, Colby R H, Giacomin A J, eds. XVth International Congress on Rheology—the Society of Rheology 80th Annual Meeting. American Institute of Physics, 2008, 994–996
76. Lee W, Walker L M, Anna S L. Role of geometry and fluid properties in droplet and thread formation processes in planar flow focusing. Physics of Fluids, 2009, 21(3): 032103
77. Anna S L. Droplets and bubbles in microfluidic devices. Annual Review of Fluid Mechanics, 2016, 48(1): 285–309
78. Garstecki P, Stone H A, Whitesides G M. Mechanism for flow-rate controlled breakup in confined geometries: A route to monodisperse emulsions. Physical Review Letters, 2005, 94(16): 164501
79. Zhou C, Yue P, Feng J J. Formation of simple and compound drops in microfluidic devices. Physics of Fluids, 2006, 18(9): 092105
80. Christopher G F, Anna S L. Microfluidic methods for generating continuous droplet streams. Journal of Physics D: Applied Physics, 2007, 40(19): R319–R336
81. Nunes J K, Tsai S S H, Wan J, Stone H A. Dripping and jetting in microfluidic multiphase flows applied to particle and fibre synthesis. Journal of Physics D: Applied Physics, 2013, 46(11):

114002–114020
82. Fu T, Wu Y, Ma Y, Li H Z. Droplet formation and breakup dynamics in microfluidic flow-focusing devices: From dripping to jetting. Chemical Engineering Science, 2012, 84: 207–217
83. Wu P, Luo Z, Liu Z, Li Z, Chen C, Feng L, He L. Drag-induced breakup mechanism for droplet generation in dripping within flow focusing microfluidics. Chinese Journal of Chemical Engineering, 2015, 23(1): 7–14
84. Utada A S, Lorenceau E, Link D R, Kaplan P D, Stone H A, Weitz D A. Monodisperse double emulsions generated from a microcapillary device. Science, 2005, 308(5721): 537–541
85. Utada A S, Fernandez-Nieves A, Stone H A, Weitz D A. Dripping to jetting transitions in coflowing liquid streams. Physical Review Letters, 2007, 99(9): 094502
86. Gañán-Calvo A M. Jetting-dripping transition of a liquid jet in a lower viscosity co-flowing immiscible liquid: The minimum flow rate in flow focusing. Journal of Fluid Mechanics, 2006, 553: 75–84
87. Deng C, Wang H, Huang W, Cheng S. Numerical and experimental study of oil-in-water (O/W) droplet formation in a co-flowing capillary device. Colloids and Surfaces A: Physicochemical and Engineering Aspects, 2017, 533: 1–8
88. Cramer C, Fischer P, Windhab E J. Drop formation in a co-flowing ambient fluid. Chemical Engineering Science, 2004, 59(15): 3045–3058
89. Suryo R, Basaran O A. Tip streaming from a liquid drop forming from a tube in a co-flowing outer fluid. Physics of Fluids, 2006, 18 (8): 082102
90. Villermaux E, Hopfinger E. Periodically arranged co-flowing jets. Journal of Fluid Mechanics, 1994, 263: 63–92
91. Wu L, Chen Y. Visualization study of emulsion droplet formation in a coflowing microchannel. Chemical Engineering and Processing: Process Intensification, 2014, 85: 77–85
92. He Y, Battat S, Fan J, Abbaspourrad A, Weitz D A. Preparation of microparticles through co-flowing of partially miscible liquids. Chemical Engineering Journal, 2017, 320: 144–150
93. Hua J, Zhang B, Lou J. Numerical simulation of microdroplet formation in coflowing immiscible liquids. AIChE Journal. American Institute of Chemical Engineers, 2007, 53(10): 2534–2548
94. Castro-hernández E, Gundabala V, Fernández-nieves A, Gordillo J M. Scaling the drop size in coflow experiments. New Journal of Physics, 2009, 11(7): 075021
95. Vladisavljevic G T, Williams R A. Manufacture of large uniform droplets using rotating membrane emulsification. Journal of Colloid and Interface Science, 2006, 299(1): 396–402
96. Joscelyne S M, Tragardh G. Membrane emulsification—a literature review. Journal of Membrane Science, 2000, 169(1): 107–117
97. Charcosset C, Limayem I, Fessi H. The membrane emulsification process—a review. Journal of Chemical Technology & Biotechnology: International Research in Process. Environmental & Clean Technology, 2004, 79(3): 209–218
98. De Luca G, Sindona A, Giorno L, Drioli E. Quantitative analysis of coupling effects in cross-flow membrane emulsification. Journal of Membrane Science, 2004, 229(1-2): 199–209
99. Drioli E, Giorno L. Membrane operations. Simulation, 2009, 1: 1
100. Sharma S, Shukla P, Misra A, Mishra P R. Chapter 8. Interfacial and colloidal properties of emulsified systems: Pharmaceutical and biological perspective. In: Colloid & Interface Science in Pharmaceutical Research & Development. Amsterdam: Elsevier, 2014, 149–172
101. Schroder V, Behrend O, Schubert H. Effect of dynamic interfacial tension on the emulsification process using microporous, ceramic membranes. Journal of Colloid and Interface Science, 1998, 202 (2): 334–340
102. Wang K, Lu Y C, Xu J H, Luo G S. Determination of dynamic interfacial tension and its effect on droplet formation in the T-shaped microdispersion process. Langmuir, 2009, 25(4): 2153–2158
103. Mozafarpour R, Koocheki A, Milani E, Varidi M. Extruded soy protein as a novel emulsifier: Structure, interfacial activity and emulsifying property. Food Hydrocolloids, 2019, 93: 361–373
104. van Dijke K, Kobayashi I, Schroen K, Uemura K, Nakajima M, Boom R. Effect of viscosities of dispersed and continuous phases in microchannel oil-in-water emulsification. Microfluidics and Nanofluidics, 2010, 9(1): 77–85
105. Wu N, Zhu Y, Leech P W, Sexton B A, Brown S, Easton C. Effects of surfactants on the formation of microdroplets in the flow focusing microfluidic device. In: Proceedings of SPIE—The International Society for Optical Engineering. Bellingham: SPIE, 2007, 6799: U84–U91
106. Vlahovska P M, Danov K D, Mehreteab A, Broze G. Adsorption kinetics of ionic surfactants with detailed account for the electrostatic interactions. Journal of Colloid and Interface Science, 1997, 192(1): 194–206
107. Sasaki M, Yasunaga T, Satake S, Ashida M. Kinetic studies on double relaxation of surfactant solutions using a capillary wave method. Bulletin of the Chemical Society of Japan, 1977, 50(12): 3144–3148
108. El-Abbassi A, Neves M A, Kobayashi I, Hafidi A, Nakajima M. Preparation and characterization of highly stable monodisperse argan oil-in-water emulsions using microchannel emulsification. European Journal of Lipid Science and Technology, 2013, 115(2): 224–231
109. Eggleton C D, Tsai T M, Stebe K J. Tip streaming from a drop in the presence of surfactants. Physical Review Letters, 2001, 87(4): 048302
110. Bracco G, Holst B. Surface Science Techniques. 1st ed. Berlin: Springer, 2013, 3–34
111. Hu S, Ren X, Bachman M, Sims C E, Li G P, Allbritton N L. Surface-directed, graft polymerization within microfluidic channels. Analytical Chemistry, 2004, 76(7): 1865–1870
112. Barrat J L, Bocquet L. Influence of wetting properties on hydrodynamic boundary conditions at a fluid/solid interface. Faraday Discussions, 1999, 112: 119–127
113. Dreyfus R, Tabeling P, Willaime H. Ordered and disordered patterns in two-phase flows in microchannels. Physical Review Letters, 2003, 90(14): 144505
114. Nie Z, Seo M, Xu S, Lewis P C, Mok M, Kumacheva E, Whitesides G M, Garstecki P, Stone H A. Emulsification in a microfluidic flow-focusing device: Effect of the viscosities of the

liquids. Microfluidics and Nanofluidics, 2008, 5(5): 585–594
115. Fournanty S, Guer Y L, Omari K E, Dejean J P. Laminar flow emulsification process to control the viscosity reduction of heavy crude oils. Journal of Dispersion Science and Technology, 2008, 29 (10): 1355–1366
116. Farokhirad S, Lee T, Morris J F. Effects of inertia and viscosity on single droplet deformation in confined shear flow. Communications in Computational Physics, 2015, 13(3): 706–724
117. Eggers R. Industrial High Pressure Applications, Processes, Equipment and Safety. 1st ed. Weinheim: Wiley-VCH Verlag & Co. KGaA, 2012, 97–122
118. Chwalek J M, Trauernicht D P, Delametter C N, Sharma R, Jeanmaire D L, Anagnostopoulos C N, Hawkins G A, Ambravaneswaran B, Panditaratne J C, Basaran O A. A new method for deflecting liquid microjets. Physics of Fluids, 2002, 14(6): L37–L40
119. Xu J H, Li S W, Tan J, Luo G S. Correlations of droplet formation in T-junction microfluidic devices: From squeezing to dripping. Microfluidics and Nanofluidics, 2008, 5(6): 711–717
120. Hong Y, Wang F. Flow rate effect on droplet control in a co-flowing microfluidic device. Microfluidics and Nanofluidics, 2007, 3(3): 341–346
121. Wright P. The variation of viscosity with temperature. Physics Education, 1977, 12(5): 323–325
122. Wengerter M, Li Y, Nieder H, Brandner J J, Schoenitz M, Scholl S. Energy and resource efficient continuous production of a binder emulsion using microstructured devices. Chemical Engineering and Processing: Process Intensification, 2017, 122: 319–329
123. Fujiu K B, Kobayashi I, Neves M A, Uemura K, Nakajima M. Effect of temperature on production of soybean oil-in-water emulsions by microchannel emulsification using different emulsifiers. Food Science and Technology Research, 2011, 17 (2): 77–86
124. Mahajan R K, Chawla J, Bakshi M S. Depression in the cloud point of Tween in the presence of glycol additives and triblock polymers. Colloid & Polymer Science, 2004, 282(10): 1165–1168
125. Shinoda K, Arai H. The correlation between phase inversion temperature in emulsion and cloud point in solution of nonionic emulsifier. Journal of Physical Chemistry, 1964, 68(12): 3485–3490
126. Shinoda K, Saito H. The stability of O/W type emulsions as functions of temperature and the HLB of emulsifiers: The emulsification by PIT-method. Journal of Colloid and Interface Science, 1969, 30(2): 258–263
127. Stan C A, Tang S K Y, Whitesides G M. Independent control of drop size and velocity in microfluidic flow-focusing generators using variable temperature and flow rate. Analytical Chemistry, 2009, 81(6): 2399–2402
128. Tice J D, Lyon A D, Ismagilov R F. Effects of viscosity on droplet formation and mixing in microfluidic channels. Analytica Chimica Acta, 2004, 507(1): 73–77
129. Nguyen N T, Ting T H, Yap Y F, Wong T N, Chai J C K, Ong W L, Zhou J, Tan S H, Yobas L. Thermally mediated droplet formation in microchannels. Applied Physics Letters, 2007, 91(8): 084102
130. Zhou Z, Kong T, Mkaouar H, Salama K N, Zhang J M. A hybrid modular microfluidic device for emulsion generation. Sensors and Actuators. A, Physical, 2018, 280: 422–428
131. Kanai T, Tsuchiya M. Microfluidic devices fabricated using stereolithography for preparation of monodisperse double emulsions. Chemical Engineering Journal, 2016, 290: 400–404